

## Detection of Nebivolol Drug Based on As-grown Un-doped Silver oxide Nanoparticles prepared by a Wet-Chemical Method

Mohammed M. Rahman<sup>1,2,\*</sup>, Sher Bahadar Khan<sup>1,2</sup>, Abdullah M. Asiri<sup>1,2</sup>, Khalid A. Alamry<sup>1,2</sup>,  
Abdulrahman O. Al-Youbi<sup>2</sup>

<sup>1</sup> Center of Excellence for Advanced Materials Research (CEAMR), King Abdulaziz University, Jeddah 21589, P.O. Box 80203, KSA

<sup>2</sup> Chemistry Department, Faculty of Science, King Abdulaziz University, P.O. Box 80203, Jeddah 21589, KSA

\*E-mail: [mmrahman@kau.edu.sa](mailto:mmrahman@kau.edu.sa); [mmrahmanh@gmail.com](mailto:mmrahmanh@gmail.com)

Received: 26 September 2012 / Accepted: 30 November 2012 / Published: 1 January 2013

---

The present study describes a simple and reliable I-V technique for detection of Nebivolol drug based on as-grown un-doped silver oxide nanoparticles at room conditions. Here, we have synthesized large-scale and low-dimensional silver oxide nanoparticles by a wet-chemical technique using reducing agents in alkaline medium. The morphological, structural, elemental, and optical properties of nanoparticles are investigated by UV/vis. and FT-IR spectroscopy, powder X-ray diffraction (XRD), X-ray photoelectron spectroscopy (XPS), and field-emission scanning electron microscopy (FESEM) etc. They were fabricated on a glassy carbon electrode (GCE) to give a fast response towards nebivolol drug. The nebivolol drug sensor also displays good sensitivity and long-term stability, and enhanced electrochemical I-V response. The calibration plot is linear ( $r^2 = 0.9294$ ) over the broad concentration range (5.46 nM ~ 99.3  $\mu$ M). The sensitivity and detection limit are calculated from the calibration plots, which are close to 3.481  $\mu$ Acm<sup>-2</sup>mM<sup>-1</sup> and 0.91 nM (Signal-to-Noise-Ratio, SNR of 3) respectively. This method could also be employed for the determination of drugs in quality control of formulation without interference of the recipients.

---

**Keywords:** Nebivolol drug, Silver oxide nanoparticles, Optical properties, I-V technique, Sensitivity, Wet-chemical method

### 1. INTRODUCTION

Nebivolol is chemically well-known as  $\alpha,\alpha'$ -[iminobis(methylene)]bis[6-flouro-3,4-dihydro-2H-1-benzopyran-2-methanol], which is high-selective  $\beta$ 1-adrenergic blocker (along-acting) with nitric oxide mediated vasodilatory actions, favorable upshots on vascular endothelial function and utilized in the controlling of hypertension [1,2]. It reduces heart rate, rate of myocardial contractility

and systemic blood-pressure, while increasing diastolic pause.  $\beta$ -blockers are useful prophylactic agents in stable and unstable types of angina. Nebivolol is a racemate (combination) of two enantiomers, SRRR-nebivolol (*d*-Nebivolol) and RSSS-nebivolol (*L*-Nebivolol). It combines two pharmacological activities, such as (a) a competitive and selective  $\beta_1$ -receptor antagonist which is attributable to the *d*-enantiomer, and (b) mild vasodilating properties, possible owing to an interaction with the *L*-arginine/nitric oxide pathway. It shows the vasodilating action that lacks of intrinsic sympathomimetic and membrane stabilizing efficiency [3]. The anti-hypertensive and anti-anginal effects of amlodipine by the calcium channel-blocking effect are featured to S-amlodipine, whereas R-amlodipine is regarded as an impurity that might be inactive or might have undesirable activities [4]. However, it is preferable in patients with bronchospasm, diabetes, peripheral vascular disease or Raynaud's phenomenon [5-7].

Silver oxide nanoparticles have attracted significant interest because of their potential applications in fabricating nano-scale electronics, optoelectronics, biological devices, electron field emission sources for emission exhibits, and the surface enhanced Raman properties [8,9]. It displays wide group of derivatives ( $\text{Ag}_2\text{O}$ ,  $\text{Ag}_2\text{O}_3$ , and  $\text{Ag}_3\text{O}_4$  etc) that attracted considerable attention, mainly owing to the widespread uses of oxides. In nanotechnology and nano-structural materials, sensors have been playing a major role in the development of very accurate, highly-sensitive, and reliable devices. The nanoparticles capable of nano-level imaging and controlling of nano-material, biological, biochemical, pathological samples have achieved the focus of interest in the scientific community [10-21]. Semiconductor nanoparticles are being comprehensively studied due to their unique surface properties conveyed by large-surface areas. Recently the development of chemical sensors based on undoped semiconductor nanostructure materials is a major goal for the detection and quantification of various toxic and hazardous chemicals [22-33]. Silver oxides are a promising semiconducting material for sensor applications due to their high chemical stability, suitability, non-toxicity, abundance in nature and low-cost, which is used in the form of single crystals, pellets, powder, and films with binders [34-48]. Thin-coating-films are more appropriate as well as adjustable for such sensors because the chemical-sensing properties are related to the material surface, where the chemicals are adsorbed/absorption. This reaction is directly depended on the concentration of charge-carriers on the un-doped semiconducting nanomaterials surfaces, which influenced to change their electrical properties (resistance, current, potential) and used for the purpose of biochemical detection [49,50].

Many techniques have been illustrated in the literature for the determination of nebivolol drug individually or in combination with other drug materials. A few analytical methods have been reported in pharmaceutical formulation, which includes UV/vis [51,52], LC-MS [53-55], HPLC [56-58] and fluorimetric [59] methods for analysis of nebivolol in biological fluids. Literature survey displays that few HPLC, UV, and colorimetric methods have been reported for evaluation of antihypertensive as single nebivolol component in bulk, formulation, and biological fluids [60-63]. Hence, the development of a new method for detecting nebivolol is urgently needed. The aim of this work is to develop drug sensors using undoped silver oxide nanoparticles by reliable I-V method with ultra-level detection for target nebivolol in pharmaceutical dosage.

Un-doped semiconductor metal oxide nanomaterial is comprehensively displayed for the detection methodology of drug biomolecules in chemical control process, due to their several benefits

over conventional chemical analysis methods. In conventional method, the uncoated nanomaterials electrodes for neбиволol detection is exhibited slower response, surface fouling, noise, unstable signals, and lower dynamic range as well as lower sensitivity. Hence, the modification of the sensor surface with undoped nanomaterials is very significant to achieve higher sensitive, repeatable, and stable responses. Therefore, a simple and reliable I-V electrochemical approach is urgently needed for relatively easy, convenient, and inexpensive instrumentation which exhibits higher sensitivity and lower detection limits compared to conventional techniques. Here, the conventional I-V method is exhibited a very reliable, large-scale, and highly sensitive detection of neбиволol drugs using undoped silver oxide nanoparticles. The present approach also depicts a sensitive, low-sample volume, ease to handle, and electrochemical techniques over the existing UV, LC-MS, and HPLC methods, which are free from complicated steps. The simple coating method for preparation of nanoparticles thin-film with conducting binders is used for the fabrication of silver oxide nanoparticles films. In present study, the low-dimensional nanoparticle is prepared with conducting binders and details investigated the neбиволol drug by simple and reliable I-V techniques. To best of our knowledge, this is the first report for highly sensitive detection of neбиволol with un-doped silver oxide nanoparticles using easy and reliable I-V method in short response time.

## 2. EXPERIMENTAL SECTIONS

### 2.1. Materials and Methods

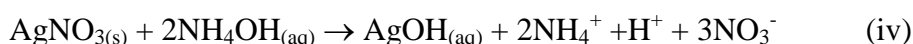
Nebivolol, butyl carbitol acetate (BCA), ethyl acetate (EA), silver nitrate, urea, ammonia solution (25%), and all other chemicals were in analytical grade and purchased from Sigma-Aldrich Company ([www.sigmaaldrich.com](http://www.sigmaaldrich.com)). Stock solutions of Nebivolol ( $C_{22}H_{25}F_2NO_4.HCl$ ; molecular weight, 441.90) were prepared by dissolving 4.388 mg in 100.0 ml of 0.1 M phosphate buffer solution (PBS) and volume was made up to mark in a 100.0 ml calibrated volumetric flask to obtain the saturated stock solution of Nebivolol drug (0.0993 mM). Morphology, size, and structure of silver oxide nanoparticles were recorded on FE-SEM instrument from JSM-7600F, Japan ([www.jeol.com](http://www.jeol.com)). FT-IR spectra were investigated on a spectrum-100 FT-IR spectrophotometer in the mid-IR range purchased from Perkin-Elmer, Germany ([www.perkinelmer.com](http://www.perkinelmer.com)). The powder X-ray diffraction patterns (XRD) were recorded by PANalytical X-ray diffractometer with  $Cu-K_{\alpha}1$  radiation ( $\lambda = 1.5406$  nm) using a generator voltage ( $\sim 45.0$  kV) and a generator current ( $\sim 40.0$  mA) were applied for the determination. The  $\lambda_{max}$  (265.0 nm) of as-grown silver oxide nanoparticles was executed using UV/visible spectroscopy Lambda-950, Perkin Elmer, Germany ([www.perkinelmer.com](http://www.perkinelmer.com)). I-V technique (two-electrode system) is employed by Kethley-Electrometer from USA ([www.keithley.com](http://www.keithley.com)).

### 2.2. Synthesis of silver oxide nanoparticles by solution method

It was prepared as-grown un-doped silver oxide nanoparticles by solution method from the reducing agents (silver nitrate and urea). Firstly, silver nitrate and urea were slowly dissolved into the

de-ionized water separately to make 0.5 M concentration at room conditions. Then the solution was mixed gently and stirred until mix properly. pH was adjusted over 9.0 by adding ammonia solution in the reaction medium. Then the mixture was placed onto the hot-plate with stirring for 6 hours. Finally, the resultant solution was washed with acetone and kept for drying at room conditions. Finally, the as-grown products were characterized in features of their structural, morphological, and optical properties as well as applied for the development of nebivolol drug sensors.

The development of silver oxide nanoparticles can be well explained based on the chemical reactions concerned and crystal growth behaviors of silver oxide. For the synthesis of silver oxide nanoparticles, silver nitrate ( $\text{AgNO}_3$ ) and  $\text{NH}_4\text{OH}$  (in presence of surfactants & urea) were mixed under continuous stirring at  $150\text{ }^\circ\text{C}$ . During growth of silver oxide nanoparticle, surfactant is used to control the size, which has significant role in reaction systems. In reaction system,  $\text{NH}_4\text{OH}$  also performs a key-rule to control the pH value of the solution and resource of hydroxyl ions to supply into the reaction system. The  $\text{AgNO}_3$  reacts with  $\text{NH}_4\text{OH}$  and forms  $\text{AgOH}$  upon heating. Further it produced  $\text{Ag}^+$  and  $\text{OH}^-$  ions, which consequently assisted in the development of silver oxides according to the chemical reactions (i) to (ii).



The  $\text{AgOH}$  finally dissociates to form of  $\text{Ag}_2\text{O}_3$  nuclei according to the reactions (iii)-(v). The nuclei of  $\text{Ag}_2\text{O}_3$  are formed gradually in the initial stage, and then it is produced the building blocks of final doped products. With reaction time under the appropriate heating conditions in solution method, the  $\text{Ag}_2\text{O}_3$  nuclei concentration enlarges which initiates the formation of desired nanoparticle products.

### 2.3. Fabrication and detection technique of nebivolol drug by nanoparticles

GCE is fabricated with as-grown silver oxide nanoparticles using butyl carbitol acetate (BCA) and ethyl acetate (EA) as a conducting binder. Then it is moved into oven (at  $60.0\text{ }^\circ\text{C}$ ) for 6 hours for drying. 0.1 M phosphate buffer solution (PBS) at pH 7.0 is prepared by mixing 0.2 M  $\text{Na}_2\text{HPO}_4$  and 0.2 M  $\text{NaH}_2\text{PO}_4$  solution in 100.0 mL de-ionize water. A cell is gathered with working (silver oxide fabricated GCE) and counter (Pd wire) electrodes. As received nebivolol is diluted to make various concentrations (5.46 nM ~ 99.3  $\mu\text{M}$ ) in PBS solution and used as a target analyte. 10.0 mL of 0.1 M PBS solution is kept constant during measurements. The ratio of voltage versus current (slope of

calibration curve) is used to measure of neбиволол sensitivity. Detection limit is measured from the ratio of  $3N/S$  versus sensitivity (ratio of noise $\times 3$  vs. sensitivity) in the linear dynamic range of calibration plot. Electrometer is used as a voltage sources for I-V measurement in simple two electrodes system. The as-grown silver oxide nanoparticles are fabricated and employed for the detection of neбиволол.

### 3. RESULTS AND DISCUSSION

#### 3.1. UV-visible and FT-IR spectroscopy

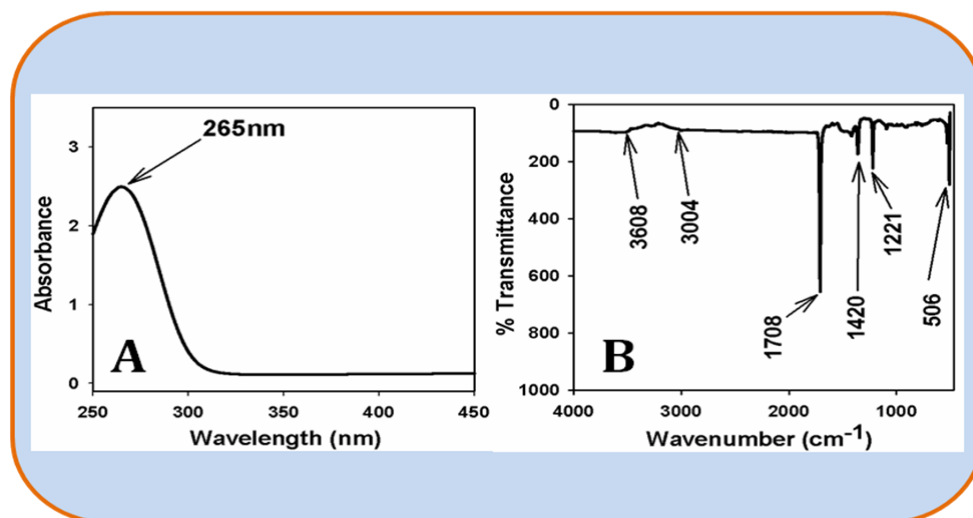


**Figure 1.** (A) UV/visible and (B) FT-IR spectroscopy of as-grown low-dimensional silver oxide nanoparticles.

The optical property of the as-grown silver oxide nanoparticles is one of the significant characteristics for the assessment of its photo-catalytic activity. In UV/visible method, the outer electrons of atoms or molecules are absorbed by the radiant energy and undergo transitions to higher energy levels. In this phenomenon, the spectrum obtained due to optical absorption can be analyzed to acquire the energy band gap of the metal oxides. For UV/visible spectroscopy, the absorption spectrum of silver oxide nanoparticles solution is measured as a function of wavelength, which is presented in Figure 1A. It presents a broad absorption band around 265.0 nm in the visible-range between 250.0 to 450.0 nm wavelengths indicating the formation of silver oxide low-dimensional nanoparticles. Band-gap energy ( $E_{bg}$ ) is calculated on the basis of maximum absorption band of silver oxide nanoparticles and found to be 4.679 eV, according to following equation.

$$E_{bg} = \frac{1240}{\lambda} \text{ (eV)}$$

Where  $E_{bg}$  is the band-gap energy and  $\lambda_{max}$  is the wavelength (265.0 nm) of the nanoparticles.

The as-prepared silver oxide nanoparticles are also studied in term of the atomic and molecular vibrations. To predict the functional-group identification, FT-IR spectra are investigated in the region of  $400 \sim 4000 \text{ cm}^{-1}$  at room conditions. Figure 1B displays the FT-IR spectrum of the nanoparticles. It represents band at  $506, 1221, 1420, 1708, 3004,$  and  $3608 \text{ cm}^{-1}$ . These observed broad vibration band (at  $506 \text{ cm}^{-1}$ ) could be assigned as metal-oxygen (Ag-O-Ag mode) stretching vibrations, which demonstrated the configuration of un-doped silver oxide nanoparticle materials. The supplementary vibrational bands may be assigned to O-H bending vibration, C-O absorption, and O-H stretching. Generally, the absorption bands are exhibited at  $1221, 1420, 1708, 3004,$  and  $3608 \text{ cm}^{-1}$  due to the presence of bending and stretching vibrations of carbon dioxide and water respectively. Usually semiconductor nanostructure materials absorb carbon dioxide and water from the environment, due to their high surface-to-volume ratio of mesoporous nature [64]. Finally, the vibrational bands at low frequencies regions are confirmed the formation of silver oxide nanoparticles by solution methods.

### 3.2. FESEM and XRD study

FE-SEM images of as-grown silver oxide nanostructure are presented in Figure 2(A-B). It exhibits the images of the spherical shapes with various dimensional sizes of as-grown silver oxide nanoparticles. The diameter of nanoparticles is calculated in the range of  $0.35 \sim 1.4 \mu\text{m}$ , where the average size is  $0.76(\pm 0.20) \mu\text{m}$ . It is clearly observed from the FE-SEM images that the prepared undoped silver oxide is nanoparticles in spherical-shape. Here it is grown in very high-density and possessing almost uniform spherical shapes.

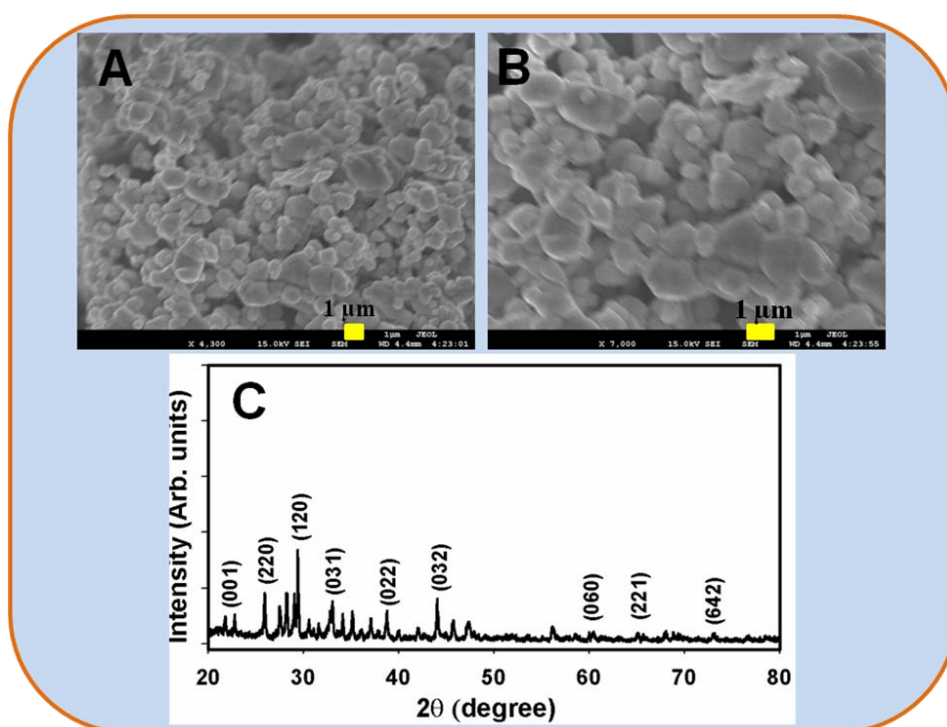


**Figure 2.** (A) FE-SEM images and (B) X-ray powder diffraction of as-grown low-dimensional silver oxide nanoparticles.

By x-ray powder diffraction, silver oxide structure (phase) in nanoparticles is compared with the standard value of lattice parameters, crystal structures, and crystallinity of JCPDS data. From the XRD data in Figure 2(C), it is clearly represented that all of the peaks match well with the Bragg reflections of the standard monoclinic ( $\text{Ag}_3\text{O}_4$ ; JC-PDF 65-9750;  $a=3.5787$ ,  $b=9.2079$ ,  $c=5.6771$ ) and face-centered orthorhombic ( $\text{Ag}_2\text{O}_3$ ; JC-PDF 77-1829;  $A=12.869$ ,  $B=10.49$ ,  $C=3.6638$ ) structures. The two-theta peaks of  $\text{Ag}_3\text{O}_4$  at  $20.2^\circ$ ,  $30.9^\circ$ ,  $38.1^\circ$ ,  $45.5^\circ$ ,  $60.1^\circ$ , and  $77.1^\circ$  can be assigned to their characteristic (001), (120), (002), (032), (060), and (311) indices respectively. The two-theta peaks of  $\text{Ag}_2\text{O}_3$  at  $22.1^\circ$ ,  $25.2^\circ$ ,  $32.6^\circ$ ,  $37.2^\circ$ ,  $44.5^\circ$ ,  $65.3^\circ$ , and  $78.1^\circ$  can be assigned to their characteristics (020), (220), (031), (111), (200), (221), and (642) indices [65]. All the reflected peaks in this pattern were found to match with JCPDF of  $\text{Ag}_3\text{O}_4$  and  $\text{Ag}_2\text{O}_3$  individually having phases with various dimensional silver oxide nanoparticles.

### 3.3. XPS analysis

X-ray photoelectron spectroscopy (XPS) is a quantitative spectroscopic method that investigates the elemental-composition, empirical-formula, chemical-state, and electronic-state of the elements that present within a material. XPS spectra are acquired by irradiating a material with a beam of X-rays, while simultaneously determining the kinetic energy and number of electrons that get-away from the top one to ten nm of the material being analyzed. Here, XPS measurements were executed for undoped as-grown silver oxide materials to investigate the chemical states of  $\text{Ag}_2\text{O}$ . The XPS spectra of Ag3d and O1s are presented in Fig. 3A.

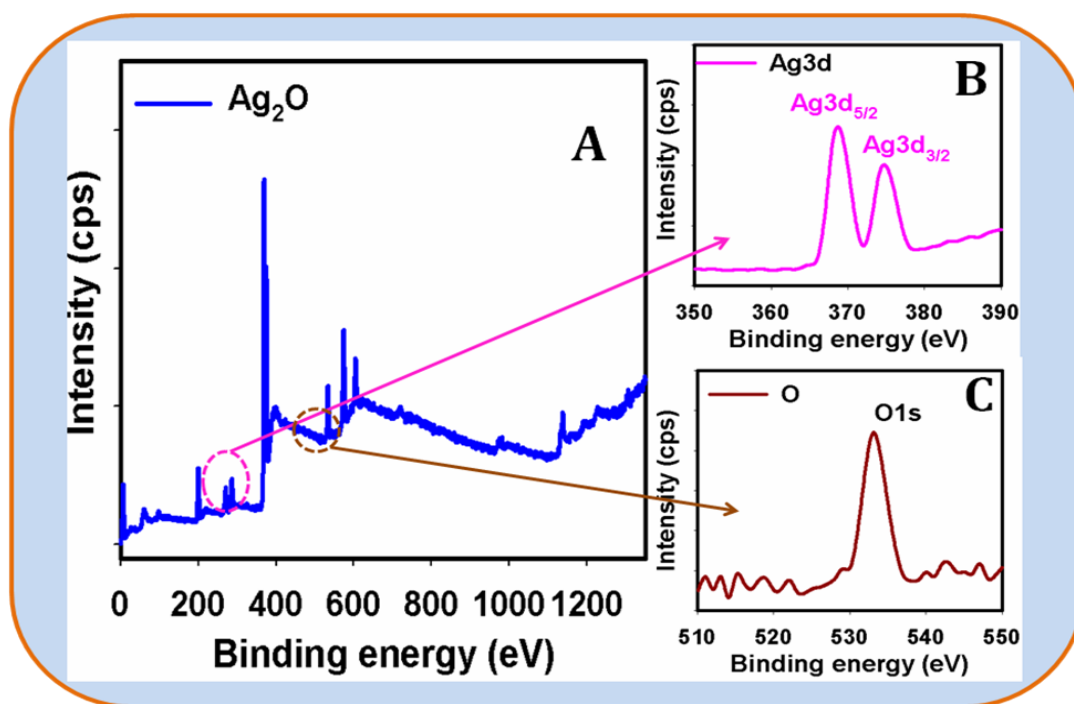


**Figure 3.** XPS of (A) undoped  $\text{Ag}_2\text{O}$  nanoparticles, (B) Ag3d level, and (C) O1s level acquired with  $\text{MgK}\alpha$  radiation.

In Figure 3B, the spin orbit peaks of the  $\text{Ag}3d_{(5/2)}$  and  $\text{Ag}3d_{(3/2)}$  binding energy for all the samples appeared at around 368.5 eV and 374.9 eV respectively, which is in good agreement with the reference data for  $\text{Ag}_2\text{O}$  [66]. The O1s spectrum shows a peak at 533.8 eV in Fig. 3C. The peak at 533.8 eV is assigned to lattice oxygen, may be indicated to oxygen (ie,  $\text{O}_2^-$ ) presence in the undoped  $\text{Ag}_2\text{O}$  nanomaterials [67].

### 3.4. In-vitro detection of Nebivolol drug using I-V technique

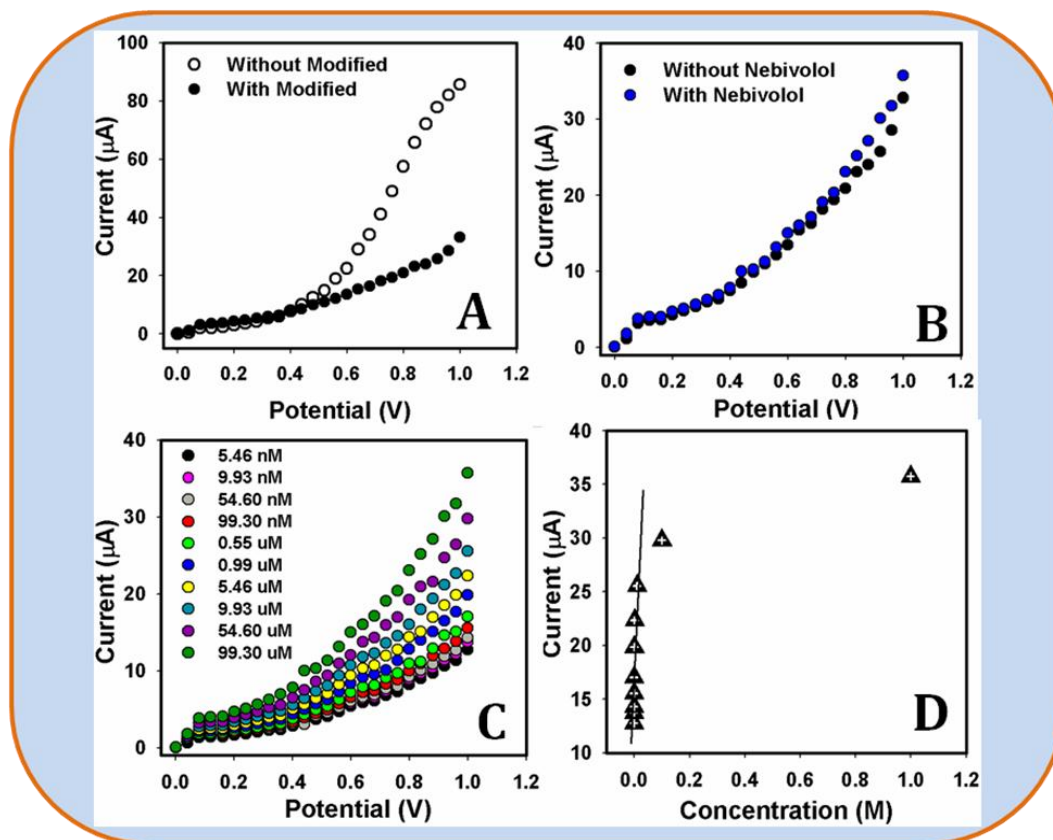
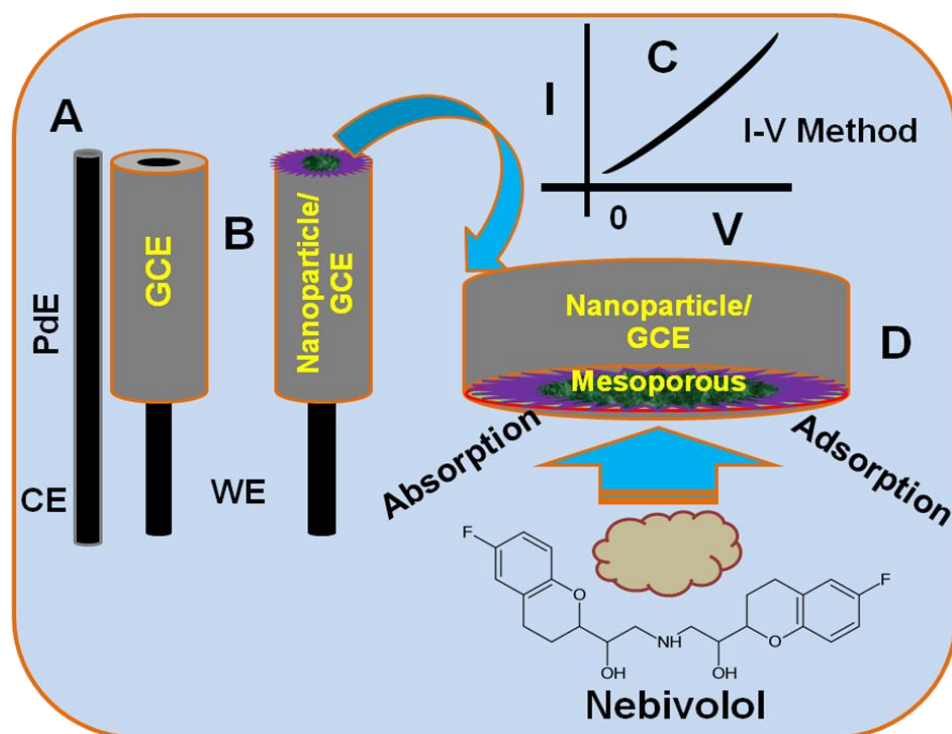


**Figure 4.** I-V responses of (A) GCE (without modified) and nanoparticles/GCE (with silver oxide modified); (B) nanoparticles/GCE (without nebigvolol) and nanoparticles/GCE (with nebigvolol); (C) Concentration variations (5.46 nM to 99.3 μM) of nebigvolol; and (D) calibration plot of nano-particles fabricated GCE.

With high mechanical strength, good conductivity, large-surface area, and particularly miniaturized size of un-doped silver oxide nanoparticles have extensively used in biomolecules and drug detection. The as-grown nanoparticles were applied for the detection of nebigvolol in liquid phase system at room conditions. Initially, the thin-film was fabricated using conducting binder and embedded on GCE. The fabrication process and detection techniques are presented in the schematic diagram (Scheme 1). The PdE and NPs fabricated GCE are used as counter and working electrodes respectively, which is presented in the Scheme 1A and Scheme 1B respectively. The nebigvolol was used as a target drug biochemical in the neutral buffer phase. The electrical responses in presence of

biochemical drugs have been measured using I-V technique according to the Scheme 1C. The physico-sorption behaviors (adsorption and absorption) as well as detection mechanism of as-grown nanoparticles are presented in the Scheme 1D. Here the nebigivolol biomolecules are absorbed as well as adsorbed onto the fabricated surfaces in huge amount, due to their mesoporous natures and large-active surface area of nanostructure material in liquid phase respectively.

The as-grown silver oxide nanoparticles were employed for the detection of nebigivolol in liquid phase. It was measured the I-V current responses (two-electrode system) based on nanoparticles modified thin-film, where GCE-electrode fabrication was already explained in experimental section. The concentration of nebigivolol was varied from 5.46 nM to 99.3  $\mu$ M by adding PBS solution at different proportion. Figure 4(A) represents the I-V responses of without (white-circle) and with (black-circle) nanoparticles coated GCE. In PBS system, the nanoparticle coated electrode exhibits that the reaction is slightly inhibited due to the presence of nanomaterials on the electrode. A significant change of current value with applied potential is clearly revealed with doped coated GCE, which is presented in Figure 4(B). The black-circle and blue-circle curves indicated the response of the nanoparticle film before and after injecting 50.0  $\mu$ L nebigivolol in 10.0 mL PBS solution respectively. A significant increase of sample current is measured after injection of target drug component in PBS system. I-V responses to varying concentration of nebigivolol on thin silver oxide nanoparticles are investigated (time delaying, 1.0 sec) and presented in the Figure 4(C). The comparative responses of resultant current of various analyte concentrations are clearly presented in Figure 4(C).



**Scheme 1.** Fabrication process and methodology of nebigivolol drug sensors using as-grown silver oxide nanoparticles. (A) Pd-counter electrode, (B) fabrication of working GC electrode, (C) expected I-V method, and (D) nebigivolol detection mechanism.

A calibration curve is plotted using current versus nebigolol concentrations to calculate the analytical parameters with fabricated sensor such as sensitivity, detection limit, linearity, and linear dynamic range etc, which is presented in Figure 4(D). A wide-range of drug concentration was chosen to study the possible detection limit (from calibration curve), which was executed in 5.46 nM to 99.3  $\mu$ M. The sensitivity was calculated from the calibration curve, which is close to  $3.481 \mu\text{Acm}^{-2}\text{mM}^{-1}$ . The linear dynamic range of the sensor was exhibited from 5.46 nM to 9.93  $\mu$ M (linearly,  $r^2 = 0.9294$ ) and the detection limit 0.91nM (at an SNR of 3). In buffer system, the drug sensing was directly related on reactant constituents, mechanism of dissociation, and further chemi-sorption of analyte on the particular silver oxide nanoparticle coated GCE surfaces. The nanomaterial coated GCE exhibits the semiconductor behaviors, where the electrical resistance is slightly decreased in presence of nebigolol drugs in reaction medium. The fabricated-film resistance is decreased gradually (increasing the resultant current) upon increasing the drug concentration in buffer phase.

**Table 1.** Comparison the performances for nebigolol drug detection based silver oxide nanoparticles using various reported methods.

Materials/Methods	LDR	LOD	Linearity (r <sup>2</sup> )	Sensitivity	Ref.
RP-HPLC	1-400 $\mu\text{g/mL}$	0.0779 $\mu\text{g/mL}$	0.9999	--	[30]
HP-TLC	500–2500 ng /spot	44.75 ng/spot	0.9978	--	[31]
UV-Visible Spectroscopy	8-80 $\mu\text{g/ml}$	0.2245 $\mu\text{g/ml}$	0.9990	--	[32]
RP-HPLC	10-30 $\mu\text{g/ml}$	14.62 ng/ml	0.9992	--	[34]
RP-HPLC	5-100 $\mu\text{g/ml}$	--	0.9999	--	[76]
RP-HPLC	5-25 $\mu\text{g/ml}$	5 $\mu\text{g/ml}$	0.9994	--	[77]
RP-HPLC	0.25-8.0 $\mu\text{g mL}^{-1}$	0.1 $\mu\text{g/mL}$	0.9997	--	[78]
UV-Visible spectrophotometry	4 -80 $\mu\text{g mL}^{-1}$	0.46 $\mu\text{g/mL}$	0.9960	--	[79]
UV/Vis. spectrophotometry	5-80 $\mu\text{g/ml}$	1.21 $\mu\text{g/ml}$	0.9985	--	[80]
Ag <sub>2</sub> O NPs/I-V	5.46 nM ~ 99.3 $\mu\text{M}$	0.91 nM	0.9294	$\sim 3.481 \mu\text{Acm}^{-2}\text{mM}^{-1}$	Current Report

The response time was approximately 10.0 sec for the silver oxide nanoparticle coated-electrode to achieve saturated steady state current. The prominent sensitivity of nebigolol drug sensor can be attributed to good absorption (porous surfaces fabricated with conducting binders) and adsorption ability (large surface area), high catalytic activity, and good biocompatibility of the un-doped nanoparticles [68-70] Due to large surface area, silver oxide nanoparticles are preferred a favorable nano-environment for the nebigolol drug detection and recognition with excellent sensitivity. The sensitivity of silver oxide nanoparticles affords high-electron communication features, which enhanced the direct electron communication between the active sites of nanoparticles and sensor electrode surfaces [71,72]. The modified thin nanoparticles coated film had a better reliability as well as stability. The un-doped nanoparticles were privileged productive surroundings for the nebigolol biomolecule detection (by adsorption) with enormous quantity, due to high dynamic and active surface area [73-75]. To check the repeatability and storage stabilities, I-V response for nanoparticle coated sensor was examined (up to 2 weeks). After each experiment, the fabricated sensor was washed

thoroughly with the PBS buffer solution and observed that the current response was not significantly decreased. The sensitivity was retained almost same of initial sensitivity up to week (1<sup>st</sup> to 2<sup>nd</sup> week), after that the response of the fabricated sensor gradually decreased. In Table 1, it is compared the performances for nebivolol drug detection based silver oxide nanoparticles using various modified electrode materials [30-32, 34, 76-80].

#### 4. CONCLUSION

Finally, the undoped silver oxide nanoparticles are prepared by a facile solution method with practically controlled structure as well as exposed a constant morphological improvement in nanostructure materials and applied for potential biomedical applications. The fabricated GCE by low-dimensional nanoparticles is observed the sensitive transduction of liquid/surface interactions for nebivolol drug detection. The structural morphology is anticipated with electrochemical approach of drug sensing biomolecules with undoped metal oxide nanostructures fabricated conventional electrodes. Here, nanoparticles are employed to fabricate a simple, efficient, and sensitive *in-vitro* nebivolol detection consisting on side-polished GCE electrode surface. To best of our knowledge, this is the first report for detection of nebivolol drug with silver oxide nanoparticles using simple and reliable I-V method in short response time. Finally, the present study has introduced a new route for the detection of nebivolol with un-doped nanoparticles with various attractive and potential features.

#### ACKNOWLEDGEMENTS

We would like to thank the Deanship of Scientific Research at King Abdulaziz University for the support of this research *via* a Research Group Track Grant (No. 3-102/428).

#### References

1. G. Carlucci, G. Palumbo, P. Mazzeo. *J. Pharm. Biomed. Anal.* 23 (2000) 185.
2. G. Carlucci, V. Carlo, P. Mazzeo. *Anal. Lett.* 33 (2000) 2491.
3. M.K. Sahoo, R.K. Giri, C.S. Barik, S.K. Kanungo, B.V.V. Ravikumar. *E-Jour. Chem.* 6 (2009) 915.
4. A. Sharma, B. Patel, R. Patel. *Inter. J. Pharma. Bio. Sci.* 1 (2010) 339.
5. P. Dhabale, D. Gharge, I.D. Gonjari, S. Kale, A.H. Arch. *Pharm. Sci. Res.* 2 (2000) 246.
6. S.C. Sweetman. *Martindale-The Complete Drug Reference*. Pharmaceutical Press: London, (36th edn), 650 (2009) 862.
7. J. Mayank, T. Sukriti, M.V. Kumar, S. Sugat, S. Saima. *Inter. J. Pharm. Life. Sci.* 1 (2010) 428.
8. Z.H. Cai, C.R. Martin. *J. Am. Chem. Soc.* 111 (1989) 4138.
9. A. Tao, F. Kim, C. Hess, J. Goldberger, R. He, Y. Sun, Y. Xia, P. Yang. *Nano. Lett.* 3 (2003) 1229.
10. P.P. Sahay, R.K. Nath. *Sens. Actuator. B* 134 (2008) 654.
11. S.R. Lee, M.M. Rahman, K. Sawada, M. Ishida. *Biosens. Bioelectron.* 24 (2009) 1877.
12. J.J. Vijaya, L.J. Kennedy, G. Sekaran, B. Jeyaraj, K.S. Nagaraja. *J. Hazard. Mater.* 153 (2008) 767.
13. S.R. Lee, M.M. Rahman, K. Sawada, M. Ishida. *Trends in Anal. Chem.* 28 (2009) 196.
14. M.M. Rahman. *J. Biomed. Nanotech.* 7 (2011) 351.
15. S.B. Khan, M.M. Rahman, K. Akhtar, A.M. Asiri, K.A. Alamry, J. Seo, H. Han. *Inter. J. Electrochem. Sci.* 7 (2012) 10965.

16. M.M. Rahman. *Sens. Transduc. J.* 126 (2011) 11.
17. S.B. Khan, M.M. Rahman, K. Akhtar, A.M. Asiri, J.C Seo, H. Han. K. Alamry. *Inter. J. Electrochem. Sci.* 7 (2012) 4030.
18. A. Umar, M.M. Rahman, S.H. Kim, Y.B. Hahn. *J. Nanosci. Nanotech.* 8 (2008) 3216.
19. M.M. Rahman. *Inter. J. Biol. Med. Res.* 1 (2010) 9.
20. M.M. Rahman, S.B. Khan, M. Faisal. A.M. Asiri, M.A. Tariq. *Electrochim. Acta* 75 (2012) 164.
21. M.M. Rahman, I.C. Jeon. *J. Organomet. Chem.* 691 (2006) 5648.
22. C. Wongchoosuk, A. Wisitsoraat, A. Tuantranont, T. Kerdcharoen. *Sens. Actuator. B* 147 (2010) 392.
23. F. Wang, S. Hu. *Microchim. Acta.* 165 (2009) 1.
24. C.C. Wang, Y.C. Weng, T.C. Chou. *Sens. Actuator. B* 122 (2007) 591.
25. A. Umar, M.M. Rahman, M. Vaseem, Y.B. Hahn. *Electrochem. Commun.* 11 (2009) 118.
26. M.M. Rahman, S.B. Khan, M. Faisal, A.M. Asiri, K.A. Alamry. *Sens. Actuator B: Chem.* 171-172 (2012) 932.
27. A. Jamal, M.M. Rahman, S.B. Khan, M. Faisal, K. Akhtar, M.A. Rub, A.M. Asiri, A.O. Al-Youbi. *App. Sur. Sci.* 261 (2012) 52.
28. A. Umar, M.M. Rahman, Y.B. Hahn. *Electrochem. Commun.* 11 (2009) 1353.
29. M.M. Rahman, A. Jamal, S.B. Khan, M. Faisal. A.M. Asiri. *Talanta* 95 (2012) 18.
30. S.B. Khan, K. Akhtar, M.M. Rahman, A.M. Asiri, J. Seo, K.A. Alamry, H. Han. *New J. Chem.* 36 (2012) 2368.
31. M.M. Rahman, A. Jamal, S.B. Khan, M. Faisal. A.M. Asiri. *Sens. Transduc. J.* 134 (2011) 32.
32. S.B. Khan, M. Faisal, M.M. Rahman, A. Jamal. *Sci. Tot. Environ.* 409 (2011) 2987.
33. M. Faisal, S.B. Khan, M.M. Rahman, A. Jamal, K. Akhtar, M.M. Abdullah. *J. Mat. Sci. Tech.* 27 (2011) 594.
34. M.M. Rahman, A. Umar, K. Sawada. *Sens. Actuat. B* 137 (2009) 327.
35. Q. Liu, J.R. Kirchoff. *J. Electroanal. Chem.* 601 (2007) 125.
36. M. Nogami T. Maeda, T. Uma. *Sens. Actuator. B: Chem.* 137 (2009) 603.
37. B. Tao, J. Zhang, S. Hui, X. Chen, L. Wan. *Electrochim. Acta* 55 (2010) 5019.
38. M.M. Rahman, A. Jamal, S.B. Khan, M. Faisal. A.M. Asiri. *Microchim. Acta* 178 (2012) 99.
39. A. Umar, M.M. Rahman, Y.B. Hahn. *Talanta* 77 (2009) 1376.
40. M. Faisal, S.B. Khan, M.M. Rahman, A. Jamal, A.M. Asiri, M.M. Abdullah. *App. Sur. Sci.* 258 (2011) 672.
41. M.M. Rahman, A. Jamal, S.B. Khan, M. Faisal. A.M. Asiri. *Chem. Engineer. J.* 192 (2012) 122.
42. A. Umar, M.M. Rahman, Y.B. Hahn. *J. Nanosci. Nanotech.* 9 (2009) 4686.
43. S.B. Khan, M.M. Rahman, E.S. Jang, K. Akhtar, H. Han. *Talanta* 84 (2011) 1005.
44. M. Faisal, S.B. Khan, M.M. Rahman, A. Jamal, A.M. Asiri, M.M. Abdullah. *App. Sur. Sci.* 258 (2012) 7515.
45. A. Umar, M.M. Rahman, A. Al-Hajry, Y.B. Hahn. *Electrochem. Commun.* 11 (2009) 278.
46. M. Faisal, S.B. Khan, M.M. Rahman, A. Jamal, A. Umar. *Mat. Lett.* 65 (2011) 1400.
47. M.M. Rahman, A. Umar, K. Sawada. *Adv. Sci. Lett.* 2 (2009) 28.
48. A. Umar, M.M. Rahman, A. Al-Hajry, Y.B. Hahn. *Talanta* 78 (2009) 284.
49. S.G. Ansari, Z.A. Ansari, R. Wahab, Y.S. Kim, G. Khang, H.S. Shin. *Biosens. Bioelectron.* 23 (2008) 1838.
50. R.R. Desai, D. Lakshminarayana, P.B. Patel, C.J. Panchal. *Sens. Actuator. B: Chem.* 107 (2005) 523.
51. M.M. Kamila, N. Mondal, L.K. Ghosh, B.K. Gupta. *Pharmazie.* 62 (2007) 486.
52. G.G. Sankar. Spectrophotometric determination of nebivolol hydrochloride Scientific Abstracts, APTI, PAR 45 (2004) 122.
53. T. Mario, O. George, S. Wilhem, *Biomed. Chromatogr.* 15 (2001) 393.

54. N.V.S. Ramakrishna, K.N. Vishwottam, M. Koteswara, S. Manoj, M. Santosh, D. Varma. *J. Pharm. Biomed. Anal.* 39 (2005) 1006.
55. H.H. Maurer, O. Tenberken, C. Kratzsch, A.A. Weber, F.T. Peters. *J. Chromatogr. A.* 1058 (2004) 169.
56. A. Annemieke, M. Marie-Jeanne, and A.V.Z. Pieter, *J. Pharmacol. Exp. Ther.* 274 (1995) 1067.
57. P.J. Pauwels, W. Gommeren, G. Van-Lommen, P.A. Janssen, J.E. Leysen, *Mol. Pharmacol.* 34 (1988) 843.
58. G. Cheymol, J.M. Poirier, P.A. Carrupt, *Br. J. Clin. Pharmacol.* 43 (1997) 563.
59. K. Rajeswari and Raja. Development of spectrofluorimetric method for the estimation of Nebivolol in tablets and human serum; Scientific Abstracts, 57th IPC, GP 69 (2005) 298.
60. J. Hendrick. M. Bock, C. Zwijsen. *J. Chromatograp.* 729 (1996) 341.
61. V. Veerasekaran, S.J. Katakdhond, S.S. Kadam. *Ind. Drug.* 38 (2001) 187.
62. The Merck-Index, Thirteenth edition, Merck Res. Lab. Division of Merck and Co. Inc, Whitehouse station, NJ. 1152 (2001) 1767.
63. B.A. Moussa, N.M. EL-Kousy. *Pharm. week. Bl. Sci.* 7 (1985) 79.
64. X. Chu, H. Zhang. *Mod. Appl. Sci.* 3 (2009) 177.
65. G.D. Wei, C.W. Nan, D.P. Yu. *Tsinghua. Sci. Technol.* 10 (2005) 736.
66. W. Wei, X. Mao, L.A. Ortiz, D.R. Sadoway. *J. Mater. Chem.* 21 (2011) 432–438.
67. M.M. Rahman, S.B. Khan, M. Faisal, M.A. Rub, A.O. Al-Youbi, A.M. Asiri. *Talanta* 99 (2012) 924-931.
68. M.M. Rahman, A. Jamal, S.B. Khan, M. Faisal. *Superlatt. Microstruc.* 50 (2011) 369.
69. A. Umar, M.M. Rahman, S.H. Kim, Y.B. Hahn. *Chem. Commun.* (2008) 166.
70. M.M. Rahman, A. Jamal, S.B. Khan, M. Faisal. *J. Nanopart. Res.* 13 (2011) 3789.
71. S.B. Khan, M. Faisal, M.M. Rahman, A. Jamal. *Talanta* 85 (2011) 943.
72. M. Faisal, S.B. Khan, M.M. Rahman, A. Jamal, A.M. Asiri, M.M. Abdullah. *Chem. Eng. J.* 173 (2011) 178.
73. M.M. Rahman, A. Jamal, S.B. Khan, M. Faisal. *Biosens. Bioelectron.* 28 (2011) 127.
74. M.M. Rahman, A. Jamal, S.B. Khan, M. Faisal. *ACS App. Mater. Interface.* 3 (2011) 1346.
75. M.M. Rahman, A. Jamal, S.B. Khan, M. Faisal. *J. Phys. Chem. C* 115 (2011) 9503.
76. B.S. Sastry, D. Srinivasulu, H. Ramana. *JPRHC.* 1 (2009) 25.
77. B. Dhandani, N.Thirumoorhy, D.J. Prakash. *E-Journal of Chemistry* 7 (2010) 341.
78. B. Yilmaz. *Inter. J. Pharm. Sci. Rev. Res.* 1 (2010)14.
79. B.C. Ankit, K.P. Rakesh, A.C. Sunita. *Int. J. Res. Pharm. Sci.* 1 (2010) 108.
80. J.S. Modiya, C.B. Pandya, K.P. Channabasavaraj. 2 (2010) 1387.